

Journal Pre-proof

Terrigenous sediment variations in the western south China sea and their implications to East Asian monsoon evolution during the last glacial-interglacial cycle

Pham Nhu Sang, Zhifei Liu



PII: S1040-6182(21)00060-4

DOI: <https://doi.org/10.1016/j.quaint.2021.02.008>

Reference: JQI 8757

To appear in: *Quaternary International*

Received Date: 2 December 2020

Revised Date: 4 February 2021

Accepted Date: 4 February 2021

Please cite this article as: Sang, P.N., Liu, Z., Terrigenous sediment variations in the western south China sea and their implications to East Asian monsoon evolution during the last glacial-interglacial cycle, *Quaternary International* (2021), doi: <https://doi.org/10.1016/j.quaint.2021.02.008>.

This is a PDF file of an article that has undergone enhancements after acceptance, such as the addition of a cover page and metadata, and formatting for readability, but it is not yet the definitive version of record. This version will undergo additional copyediting, typesetting and review before it is published in its final form, but we are providing this version to give early visibility of the article. Please note that, during the production process, errors may be discovered which could affect the content, and all legal disclaimers that apply to the journal pertain.

© 2021 Published by Elsevier Ltd.

Terrigenous sediment variations in the western South China Sea and their implications to East Asian monsoon evolution during the last glacial-interglacial cycle

Pham Nhu Sang^a, Zhifei Liu^{a,*}

^aState Key Laboratory of Marine Geology, Tongji University, Shanghai 20092, China

*Corresponding author

E-mail address: lzhifei@tongji.edu.cn

Abstract

Major-element geochemistry from two Cores MD05-2899 and MD05-2901 off central Vietnam in the lower continental slope of the western South China Sea is investigated to reconstruct a history of terrigenous sediment variations and East Asian monsoon evolution during the last glacial-interglacial cycle. The results suggest that the Pearl River can play a more important role in contributing terrigenous sediments to the western South China Sea than the Red River in the north, while the Mekong River can transport more terrigenous sediments to the region than the Sunda shelf and the Indonesian islands in the south. The Pearl River provides terrigenous sediments with higher Al_2O_3 , but lower K_2O , MgO , and Fe_2O_3 (Total Fe) than the Mekong River. $\text{K}_2\text{O}/\text{Al}_2\text{O}_3$, $\text{MgO}/\text{Al}_2\text{O}_3$, and $\text{Fe}_2\text{O}_3/\text{Al}_2\text{O}_3$ ratios are then used as proxies to trace terrigenous sediment variations in the western South China Sea. Higher $\text{K}_2\text{O}/\text{Al}_2\text{O}_3$, $\text{MgO}/\text{Al}_2\text{O}_3$, and $\text{Fe}_2\text{O}_3/\text{Al}_2\text{O}_3$ ratios indicate strengthened terrigenous sediments input from the southern source and lower the ratios suggest increased terrigenous sediments received from the northern source. These ratios show a glacial-interglacial cycle over the past 130 ka, implying a close relationship with the East Asian monsoon evolution. Northward surface currents forced by strengthened summer monsoon during interglacial periods bring relatively higher amounts of terrigenous sediments from the southern source to the western South China Sea, while

relatively higher amounts of terrigenous sediments from the northern source are transported to the western South China Sea by southward surface currents in strengthened winter monsoon during glacial periods. Our study indicates that the terrigenous sediment variations in the western South China Sea are significantly controlled by surface currents under the strong influence of the East Asian monsoon evolution during the last glacial-interglacial cycle.

Keywords: Major-element geochemistry; Terrigenous sediments; Last glacial-interglacial cycle; East Asian monsoon; Western South China Sea

1. Introduction

The East Asian monsoon system is a significant component of both the global as well as the regional climatic system, and it controls the summer and winter monsoon winds, seasonal precipitation, and runoff regimes over Southeast Asia (Webster, 1994). The East Asian monsoon is characterized by seasonal changes in wind patterns, temperature, and moisture (Chu and Wang, 2003). In summer, the monsoon can bring warmer and higher moisture from the ocean to the continent, whilst in winter it can cause the land colder and drier. The East Asian monsoon evolution strongly impacts the weathering process on the land, and the biological process and paleoenvironmental evolution in the sea (Jian et al., 2001; Liu et al., 2003, 2004, 2007a, 2012; Wan et al., 2007; Colin et al., 2010; Clift et al., 2014). Therefore, marine sediments contain significant information to be widely used for investigating the influence of the East Asian monsoon evolution at different geological timescales. The South China Sea is the largest marginal sea in the western Pacific, and surface-water circulations in this area are strongly forced by the East Asian monsoon evolution (Wang et al., 1995; Fig. 1). Generally, surface currents in the South China Sea are seasonal; the northward surface currents are strongly forced by the summer monsoon, while the southward surface currents are significantly controlled by the winter monsoon. The pathways of suspended sediment transports

in the South China Sea can be changed by the impacts of the surface currents following seasonal wind patterns (Liu et al., 2003, 2007b, 2016). The western South China Sea is encompassed by South China to the north, the Indochina Peninsula to the west, and the Malay Peninsula and Sumatra to the south (Fig. 1). This area receives larger amounts of suspended sediments by numerous surrounding rivers including several of the world's largest rivers (i.e., the Mekong River, the Red River, and the Pearl River) (Milliman and Farnsworth, 2011; Liu et al., 2016). Following Liu et al. (2016), clay minerals in the western South China Sea mainly originate from the Mekong River, the Indonesian island, and the Sunda shelf in the south and the Pearl River and the Red River in the north. Furthermore, variation in clay minerals in this area showed a close relationship with glacial-interglacial cyclicity. The western South China Sea is consequently an ideal area to investigate terrigenous sediment variations under the influence of the East Asian monsoon evolution.

In the South China Sea, elemental geochemistry of terrigenous sediments plays a significant role in investigating terrigenous sediment variations and the East Asian monsoon evolution (Liu et al., 2004; Colin et al., 2010; Clift et al., 2014; Jiwarungrueangkul et al., 2019a, 2019b; Sang et al., 2019). This suggests that major-element geochemistry of terrigenous sediments in the western South China Sea can reflect a history of terrigenous sediment variations and East Asian monsoon evolution. This study intends to investigate the sources and geochemical characteristics of terrigenous sediments through analyzing two sediment cores (MD05-2899 and MD05-2901) off central Vietnam in order to reconstruct the East Asian monsoon evolution during the last glacial-interglacial cycle.

2. Material and methods

Cores MD05-2899 (13°47.66'N, 112°10.89'E, water depth 2,393 m, core length 36.68 m) and MD05-2901 (14°22.50'N, 110°44.60'E, water depth 1,454 m, core length 36.49 m) were collected off central Vietnam in the lower continental slope of the western South China Sea

during the cruise MARCO POLO in 2005 (Laj et al., 2005; Fig. 1). The upper parts of two cores (upper 12.97 m for MD05-2899 and upper 13.50 m for MD05-2901) were used in this study in order to focus on the temporal interval of the last glacial-interglacial cycle. A total of 377 samples (216 samples from MD05-2899 with a depth resolution of 6 cm and 161 samples from MD05-2901 with a depth resolution of 8 cm) were analyzed for major element geochemistry. Age models of these two cores were established by carbonate stratigraphy and oxygen isotope stratigraphy of planktonic foraminifera *G. ruber* (Liu et al., 2007b; He et al., 2012).

Major elements were measured on bulk sediments by X-ray fluorescence (XRF) using a PANalytical Axios^{MAX} spectrometer at the State Key Laboratory of Marine Geology, Tongji University. Samples were air-dried and finely ground to powder with an agate mortar and pestle. About 4 g of the powder was mixed with H₃BO₃ as a substrate in a set of cylinder mold and then compressed under 40 MPa to obtain a pellet for analysis. Analytical precision and accuracy were monitored by measurements of national geostandards GSR-6 and GSD-15 provided by the National Research Center for Geoanalysis of marine sediments. Major-element oxides (i.e., SiO₂, Al₂O₃, Fe₂O₃, MgO, CaO, K₂O, Na₂O, P₂O₅, TiO₂, and MnO) were used to report the data.

3. Results

Major elements of Cores MD05-2899 and MD05-2901 mainly contain SiO₂, Al₂O₃, Fe₂O₃, and CaO (totally about 74%), with low concentrations of MgO, K₂O, Na₂O, P₂O₅, TiO₂, and MnO (totally about 8%) (Figs. 2 and 3; Supplementary Materials). In Core MD05-2899, SiO₂, Al₂O₃, Fe₂O₃, MgO, K₂O, and TiO₂ concentrations display inverse correlations to CaO and P₂O₅. The SiO₂, Al₂O₃, Fe₂O₃, MgO, K₂O, and TiO₂ contents have high values with little variability during the Marine Isotope Stage (MIS) 5 and low values from MIS 2–4 to the present. The CaO and P₂O₅ contents are characterized by low values with little variability during MIS 5 and increased values from MIS 2–4 to the present. However, variations in the Na₂O and MnO contents show a different pattern to other oxides. The Na₂O content doesn't display a significant difference

between glacial and interglacial periods, while the MnO content displays increased values from early to end of MIS 5, then decreased values from MIS 4 to middle MIS 1, and finally increased values to the present.

In Core MD05-2901, SiO_2 , Al_2O_3 , Fe_2O_3 , MgO , K_2O , and TiO_2 are generally inversely correlated with CaO , and their contents exhibit increased values during MIS 5 and 1 and decreased values during MIS 6 and 2–4. On the contrary, the CaO content shows decreased values during MIS 5 and 1 and increased content during MIS 6 and 2–4. Downcore variations of Na_2O , P_2O_5 , and MnO contents, however, show different patterns from the other oxides, unrelating to the glacial-interglacial cyclicity. The Na_2O and MnO contents display insignificant variability during glacial and interglacial periods, while the P_2O_5 content shows little variability from MIS 6 to the present.

4. Discussion

To investigate terrigenous sediment variations and their implications for paleoenvironmental evolution in the South China Sea, it is necessary to document potential sources and transport processes of terrigenous sediments (Liu et al., 2004, 2005, 2007b, 2016; Huang et al., 2016). Generally, the large rivers can supply much sediment discharge to the South China Sea such as the Mekong River (166 Mt/yr), the Red River (138 Mt/yr), and the Pearl River (102 Mt/yr) (Milliman and Syvitski, 1992; Milliman and Farnsworth, 2011; Zhang et al., 2012). In the western South China Sea, terrigenous sediments can be mainly provided by the Mekong River, the Sunda shelf and the Indonesian islands in the south, and the Pearl and Red rivers in the north. Eolian dust contribution to the western South China Sea could be ignored based on previous studies on terrigenous clay minerals in this area (Liu et al., 2003, 2004), e.g., on Core MD05-2901 (Liu et al., 2007b). Considering small drainage area, short length, and little sediment discharge from small mountainous rivers in central Vietnam (Liu et al., 2016), our study also believes that central Vietnam cannot contribute a valuable amount of terrigenous sediments to

the lower continental slope of the western South China Sea. Therefore, the western South China Sea can principally receive terrigenous sediments from important sources in the north and the south.

Terrigenous sediment variations can be generally controlled by the weathering process in the source region under the influence of lithology, climate condition, and tectonic activity, but major element geochemistry of terrigenous sediments in the western South China Sea can mainly reflect changes in sediment sources between glacial and interglacial periods. The chemical weathering causes depletion of mobile elements (e.g., K, Na, Mg, and Ca) and enrichment of immobile elements (e.g., Al, Fe, and Ti) in weathering products (Nesbitt et al., 1980). The behavior of major elements during the chemical weathering on the Earth's surface can be conserved in sediments and they have been widely utilized to identify the altered pathway and to evaluate the intensive chemical weathering in the source region. Furthermore, the weathering process in the source region is significantly influenced by lithology, climate condition, and tectonic activity. This implies that parent rocks in different river drainage basins can be undergone by different weathering conditions and their elemental geochemistry can be presented by special features. To display the representation of elemental geochemistry in the studied area, chemical index of alteration (CIA), $\text{Al}_2\text{O}_3 - (\text{CaO} + \text{Na}_2\text{O}) - \text{K}_2\text{O}$ (A-CN-K), and $\text{Al}_2\text{O}_3 - (\text{CaO}^* + \text{Na}_2\text{O} + \text{K}_2\text{O}) - (\text{Fe}_2\text{O}_3 + \text{MgO})$ (A-CNK-FM) diagrams are employed in this study. CIA value is utilized to estimate the intensity of chemical weathering and it is calculated by the molar weight ratios of major oxides, $\text{CIA} = [\text{Al}_2\text{O}_3 / (\text{Al}_2\text{O}_3 + \text{CaO}^* + \text{Na}_2\text{O} + \text{K}_2\text{O})] \times 100$, where CaO^* is the amount of CaO incorporated in the silicate fraction (Nesbitt and Young, 1982, 1989; McLennan, 1993; Nesbitt et al., 1996).

All samples of Cores MD05-2899 and MD05-2901 are here grouped into two intervals: interglacial and glacial samples. The CIA values recorded in Core MD05-2899 are 62.2–68.3 (average 65.1) with 62.2–67.4 for the interglacial interval and 63.1–68.3 for the glacial interval. The CIA values of Core MD05-2901 vary in the range of 60.8–70.4 (average 66.1) with 60.8–

70.4 for the interglacial interval and 63.0–70.2 for the glacial interval (Figs. 4A and 5). Core MD05-2901 has similar CIA values to Core MD05-2899, implying that their source rock region could be influenced by similar weathering conditions or they are the same sediment sources. In general, the glacial interval of both cores displays higher CIA values than the interglacial interval (Figs. 4 and 5), suggesting that variations in CIA value in this studied area cannot express the influence of synchronous climate conditions between glacial and interglacial periods on the weathering process in the source region. Because interglacial periods are usually characterized by warm and humid climate conditions which should increase the chemical weathering in the source region, while glacial periods are frequently represented by cold and dry climate conditions which allow encouragingly developing the physical weathering. This means that variations in CIA value in this area can be highly impacted by changes in sediment sources instead of synchronous climate conditions in the source region (Fig. 5).

Furthermore, weathering trends can be normally investigated based on A-CN-K and A-CN-K-FM ternary diagrams (Nesbitt and Young, 1984, 1989). All interglacial and glacial samples in two cores are lesser closes to the Al_2O_3 apex than reference data of the Pearl, Mekong, and Red rivers (Liu et al., 2007a) and Sumatra rivers (Liu et al., 2012; Fig. 4). Generally, cold and dry climate conditions during glacial periods caused weaker movement of mobile elements in weathering products than during interglacial periods. However, glacial samples show stronger leaching of elements (i.e., Ca, Na, K, Mg, Fe) than interglacial samples (Fig. 4), suggesting that movement of major elements in the A-CN-K and A-CN-K-FM ternary diagrams can reflect variations in sediment sources between glacial and interglacial periods instead of synchronous weathering trends in the source region. Therefore, all variations in CIA value and movement of major elements in the A-CN-K, and A-CN-K-FM ternary diagrams of both Cores MD05-2899 and MD05-2901 in the western South China Sea could be significantly forced by changes in sediment sources between glacial and interglacial periods.

In the western South China Sea, the southward surface currents can bring terrigenous sediments from the Pearl and Red rivers in the north, while the northward surface currents can transport terrigenous sediments from the Mekong River, the Sunda shelf, and the Indonesian islands in the south (Fig. 1). In the north, the Pearl River shows stronger chemical weathering states than in the Red River, implying higher CIA values and more depletion of major elements in the Pearl River, while the chemical weathering intensity in the Mekong River displays a weaker degree than in the Indonesian islands in the south, suggesting lower CIA values and lesser leaching of major elements in the Mekong River (Liu et al., 2007a, 2012; Fig. 4). Additionally, parent rocks in the Pearl River have been undergone by stronger chemical weathering than in the Mekong River, indicating higher CIA values and enhanced movement of major elements in the Pearl River (Fig. 4). Considering higher CIA values and stronger movements of major elements in the A-CN-K, and A-CNK-FM ternary diagrams for Cores MD05-2899 and MD05-2901 during the glacial interval than the interglacial interval, we believe that in the northern source the Pearl River can supply higher terrigenous sediments than the Red River to the western South China Sea, while in the south the Mekong River can contribute more terrigenous sediments to this studied area than the Indonesian islands and the Sunda shelf. This also indicates that the northern source can be principally represented by terrigenous sediments from the Pearl River, and terrigenous sediments in the Mekong River can reflect special features of the southern source.

Reference data of the Pearl River is closer to the Al_2O_3 apex than reference data of the Mekong River (Fig. 4), suggesting that the Pearl River can contain terrigenous sediments with higher Al_2O_3 , but lower K_2O , MgO , and Fe_2O_3 than the Mekong River. This may also be supported by clay mineral contents in these rivers due to the Mekong River can provide more illite ($(\text{K}_x\text{Al}_2(\text{Si}_{4-x}\text{Al}_x)\text{O}_{10}(\text{OH})_2$) and chlorite ($(\text{Mg,Fe})_5(\text{Al,Fe})_2\text{Si}_3\text{O}_{10}(\text{OH})_8$) with higher K_2O , MgO , and Fe_2O_3 contents in the sediments, while the Pearl River consists mainly of kaolinite ($\text{Al}_2\text{Si}_2\text{O}_5(\text{OH})_4$), including enrichment the sediment with Al_2O_3 (Chamley, 1989; Li and

Schoonmaker, 2003; Liu et al., 2007a) and the lower continental slope of the western South China Sea may mostly receive fine-grained materials primarily mainly of clay minerals owing to the cores' distance from their sediment sources (Fig. 1). Therefore, K_2O/Al_2O_3 , MgO/Al_2O_3 , and Fe_2O_3/Al_2O_3 ratios can be used to evaluate the relative proportion of terrigenous sediments from the Pearl River in the north versus terrigenous sediments from the Mekong River in the south. Hence, these ratios at both Cores MD05-2899 and MD05-2901 are useful proxies for reconstructing the history of terrigenous sediment input in the western South China Sea during the last glacial-interglacial cycle (Fig. 5). Higher K_2O/Al_2O_3 , MgO/Al_2O_3 , and Fe_2O_3/Al_2O_3 ratios would correspond to increased terrigenous sediment input from the southern source, while lower ratios imply enhanced terrigenous sediments from the northern source. In Cores MD05-2899 and MD05-2901, the K_2O/Al_2O_3 , MgO/Al_2O_3 , and Fe_2O_3/Al_2O_3 ratios display similar changes following the glacial-interglacial cyclicity over the past 130 ka, suggesting a close relationship between terrigenous sediment variations and East Asian monsoon evolution.

During the glacial MIS 6, the East Asian monsoon was characterized by strengthened winter monsoon and weakened summer monsoon, causing stronger southward surface currents in the western South China Sea. The southward surface currents could relatively transport higher terrigenous sediments from the northern source to the western South China Sea that is indicated by the relatively low 0.193–0.200 K_2O/Al_2O_3 , 0.169–0.194 MgO/Al_2O_3 , and 0.348–0.384 Fe_2O_3/Al_2O_3 ratios at Core MD05-2901 (Fig. 5). Variations in these geochemical proxies display a correspondence with planktonic foraminifera *G. ruber* $\delta^{18}O$ records and a mineralogical indicator ((illite + chlorite)/kaolinite) of the East Asian monsoon evolution at Core MD05-2901 (Liu et al., 2007b). At the end of this period, increases in these ratios could concern with changes in sediment sources, implying that the southern source could supply more terrigenous sediments to the western South China Sea after this stage. This phenomenon could closely relate to abundant summer monsoon and prevailing northward surface currents in this studied area during the interglacial MIS 5.

During the interglacial MIS 5, the East Asian monsoon displayed stronger summer monsoon and weaker winter monsoon, resulting in strengthened northward surface currents in the western South China Sea. The northward surface currents relatively brought higher terrigenous sediments from the southern source to the region inferred by the relatively high 0.200–0.218 K_2O/Al_2O_3 , 0.178–0.211 MgO/Al_2O_3 , and 0.381–0.462 Fe_2O_3/Al_2O_3 ratios at Core MD05-2899 and 0.200–0.219 K_2O/Al_2O_3 , 0.193–0.208 MgO/Al_2O_3 , and 0.383–0.424 Fe_2O_3/Al_2O_3 ratios at Core MD05-2901 (Fig. 5). In this period, variations in the proxies also correspond well to the planktonic foraminiferal $\delta^{18}O$ and (illite + chlorite)/kaolinite records at Core MD05-2901 (Liu et al., 2007b). After this period, the elemental proxies showed evident decreasing trends, deducing changes in sediment sources with higher terrigenous sediment contribution from the northern source during the last glacial MIS 2–4. This could be caused by a stronger winter monsoon that raised predominant southward surface currents in the western South China Sea.

During the last glacial MIS 2–4, the East Asian monsoon was represented by increased winter monsoon and decreased summer monsoon, indicating enhanced southward surface currents in the western South China Sea. Apparent phase changes in sediment sources could be observed between the glacial MIS 4, 3, and 2, relating mainly to variations of the surface currents in the western South China Sea under the significant influence of the East Asian monsoon evolution.

During the last glacial MIS 4, the southward surface currents in this studied area could encourage the relatively higher terrigenous sediments from the northern source suggested by the relatively reduced 0.201–0.215 K_2O/Al_2O_3 , 0.170–0.210 MgO/Al_2O_3 , and 0.363–0.440 Fe_2O_3/Al_2O_3 ratios at Core MD05-2899 and 0.200–0.213 K_2O/Al_2O_3 , 0.180–0.196 MgO/Al_2O_3 , and 0.368–0.400 Fe_2O_3/Al_2O_3 ratios at Core MD05-2901 (Fig. 5). Variations in the geochemical proxies also show a close relationship with the planktonic foraminiferal $\delta^{18}O$ and (illite +

chlorite)/kaolinite ratio records at Core MD05-2901 in this period. At the end of this period, all of the proxies still displayed evident decreasing trends, suggesting that the northern source contributed higher terrigenous sediment to the western South China Sea under influence of stronger southward surface currents after the last glacial MIS 4.

During the last glacial MIS 3, the southward surface currents transported the relatively higher terrigenous sediment from the northern source indicated by the relatively decreased 0.193–0.204 K_2O/Al_2O_3 , 0.157–0.194 MgO/Al_2O_3 , and 0.348–0.412 Fe_2O_3/Al_2O_3 ratios at Core MD05-2899 and 0.188–0.203 K_2O/Al_2O_3 , 0.159–0.186 MgO/Al_2O_3 , and 0.339–0.388 Fe_2O_3/Al_2O_3 ratios at Core MD05-2901 (Fig. 5). Around 38.6 ka (a red dashed line), an evident increase of all the elemental ratios could display clear changes in sediment sources with higher sediment contribution from the southern source which were principally concerned with enhanced summer monsoon as well as abundant northward surface currents in this studied area. After that, all of the ratios decreased relating to changes in sediment sources again with higher terrigenous sediment from the northern source. Variations in the geochemical proxies are similar to the planktonic foraminiferal $\delta^{18}O$ and (illite + chlorite)/kaolinite ratio records at Core MD05-2901. These elemental ratios were the lowest values after the last glacial MIS 3, indicating the highest sediment contribution from the northern source that could significantly relate to abundant southward surface currents during the last glacial MIS 2.

During the last glacial MIS 2, the strongest southward surface currents could bring the relatively highest terrigenous sediment from the northern source to the studied area implied by the relatively lowest 0.191–0.198 K_2O/Al_2O_3 , 0.152–0.183 MgO/Al_2O_3 , and 0.336–0.417 Fe_2O_3/Al_2O_3 ratios at Core MD05-2899 and 0.187–0.193 K_2O/Al_2O_3 , 0.154–0.175 MgO/Al_2O_3 , and 0.345–0.379 Fe_2O_3/Al_2O_3 ratios at Core MD05-2901 (Fig. 5). In this period, variations in the geochemical proxies positively correlate with the planktonic foraminiferal $\delta^{18}O$ and (illite + chlorite)/kaolinite ratio records at Core MD05-2901. At the end of the last glacial, changes in

sediment sources could be recognized by the generally increasing ratios. The southern source could transport higher terrigenous sediments to this studied area, concerning with enhanced northward surface currents, which were significantly forced by abundant summer monsoon during the Holocene. During the Holocene MIS 1, the East Asian monsoon presented enhanced summer monsoon and weakened winter monsoon, causing increased northward surface currents in the western South China Sea. The region has been supplied higher terrigenous sediments from the southern source under the impact of the northward surface currents as implied by the relatively increased $0.186\text{--}0.200$ $\text{K}_2\text{O}/\text{Al}_2\text{O}_3$, $0.158\text{--}0.203$ $\text{MgO}/\text{Al}_2\text{O}_3$, and $0.365\text{--}0.478$ $\text{Fe}_2\text{O}_3/\text{Al}_2\text{O}_3$ ratios at Core MD05-2899 and $0.190\text{--}0.196$ $\text{K}_2\text{O}/\text{Al}_2\text{O}_3$, $0.172\text{--}0.192$ $\text{MgO}/\text{Al}_2\text{O}_3$, and $0.363\text{--}0.400$ $\text{Fe}_2\text{O}_3/\text{Al}_2\text{O}_3$ ratios at Core MD05-2901 (Fig. 5). However, not all of the elemental ratios displayed apparent differences between the Holocene (MIS 1) and the last glacial MIS 2–4, except the $\text{MgO}/\text{Al}_2\text{O}_3$ ratio. This is because K, Mg, and Fe elements generally show different behavior during the chemical weathering in the source regions and they just presented similar variations in their contents (Figs. 2 and 3). As a result, $\text{K}_2\text{O}/\text{Al}_2\text{O}_3$, $\text{MgO}/\text{Al}_2\text{O}_3$, and $\text{Fe}_2\text{O}_3/\text{Al}_2\text{O}_3$ ratios only displayed similar patterns during the last glacial-interglacial cycle. Nevertheless, variations in these proxies also show a correspondence with the planktonic foraminiferal $\delta^{18}\text{O}$ and (illite + chlorite)/kaolinite at Core MD05-2901 during the Holocene.

For both Cores MD05-2899 and MD05-2901, the geochemical proxies ($\text{K}_2\text{O}/\text{Al}_2\text{O}_3$, $\text{MgO}/\text{Al}_2\text{O}_3$, and $\text{Fe}_2\text{O}_3/\text{Al}_2\text{O}_3$) are valuable indicators for reconstructing the history of terrigenous sediment variations under the influence of seasonal surface currents, which are significantly related to the East Asian monsoon evolution (Fig. 5). Generally, the $\text{K}_2\text{O}/\text{Al}_2\text{O}_3$, $\text{MgO}/\text{Al}_2\text{O}_3$, and $\text{Fe}_2\text{O}_3/\text{Al}_2\text{O}_3$ ratios and the mineralogical indicator ((illite + chlorite)/kaolinite) of the East Asian monsoon evolution in the western South China Sea from Liu et al. (2007b) are well correlated in certain intervals (Fig. 5). These proxies display an evident glacial-interglacial cyclicity with higher values during interglacial periods and lower values during glacial periods. Furthermore, variations in these proxies also display a strong inverse correlation to planktonic foraminifera G.

ruber $\delta^{18}\text{O}$ record fluctuations of Core MD05-2901 (Liu et al., 2007b; Fig. 5). These indicate that the East Asian monsoon system significantly causes seasonal surface currents which mainly control terrigenous sediment variations in the western South China Sea. During glacial periods, strengthened winter monsoon can more strongly force the southward surface currents to relatively bring higher terrigenous sediments from the northern source to the western South China Sea, while enhanced summer monsoon during interglacial periods can cause stronger the northward surface currents to relatively transport more terrigenous sediments from the southern source to the western South China Sea.

5. Conclusions

Major-element geochemistry of the sediments from Cores MD05-2899 and MD05-2901 in the lower continental slope of the western South China Sea were used to investigate a history of terrigenous sediment variation and East Asian monsoon evolution during the last glacial-interglacial cycle. This research concludes that:

(1) The western South China Sea can receive more terrigenous sediments from the Pearl River than the Red River in the north, while the Mekong River can transport more terrigenous sediments to this studied area than the Sunda shelf and the Indonesian islands in the south. The Pearl River can supply terrigenous sediments with higher Al_2O_3 , but lower K_2O , MgO , and Fe_2O_3 than the Mekong River to the western South China Sea.

(2) $\text{K}_2\text{O}/\text{Al}_2\text{O}_3$, $\text{MgO}/\text{Al}_2\text{O}_3$, and $\text{Fe}_2\text{O}_3/\text{Al}_2\text{O}_3$ ratios are utilized as efficient geochemical proxies in reconstructing the history of terrigenous sediment variations and the East Asian monsoon evolution in the western South China Sea. Relatively higher $\text{K}_2\text{O}/\text{Al}_2\text{O}_3$, $\text{MgO}/\text{Al}_2\text{O}_3$, and $\text{Fe}_2\text{O}_3/\text{Al}_2\text{O}_3$ ratios suggest increased terrigenous sediments input from the southern source and strengthened the East Asian summer monsoon during interglacial periods, and a relative decrease of the ratios refers to more terrigenous sediment input from the northern source, as well as enhanced the East Asian winter monsoon during glacial periods.

(3) K_2O/Al_2O_3 , MgO/Al_2O_3 , and Fe_2O_3/Al_2O_3 ratios indicate a strong glacial-interglacial cyclicity over the past 130 ka, suggesting that terrigenous sediment variations in the western South China Sea have been mainly controlled by seasonal surface currents under the significant influence of the East Asian monsoon evolution.

Acknowledgments

We would like to thank the crew and scientists on board the R/V *Marion Dufresne* for collecting sediment cores during the cruise IMAGES-MARCO POLO in 2005. We also thank Yanli Li, Juan Xu, and Xiantong Huang for their assistance in managing the X-ray fluorescence (XRF) laboratory analysis and Thanakorn Jiwrungrueangkul for valuable discussions. We especially thank Jule Xiao and an anonymous reviewer for their constructive reviews on the early version of this paper. This work was supported by the Shanghai International Science and Technology Cooperation Fund (19230742100), the National Key R&D Program of China (2018YFE0202402), and the National Natural Science Foundation of China (41530964).

Appendix A. Supplementary materials

Major element concentrations of Cores MD05-2899 and MD05-2901 in the western South China Sea during the last glacial-interglacial cycle.

References

- Chamley, H., 1989. Clay sedimentology. Springer, New York, pp. 263. <https://doi.org/10.1007/978-3-642-85916-8>.
- Chu, P.C., Wang, G., 2003. Seasonal variability of thermohaline front in the Central South China Sea. *Journal of Oceanography* 59, 65–78. <https://doi.org/10.1023/A:1022868407012>.
- Clift, P.D., Wan, S., Blusztajn, J., 2014. Reconstructing chemical weathering, physical erosion and monsoon intensity since 25 Ma in the northern South China Sea: A review of

- competing proxies. *Earth-Science Reviews* 130, 86–102.
<https://doi.org/10.1016/j.earscirev.2014.01.002>.
- Colin, C., Siani, G., Sicre, M.A., Liu, Z., 2010. Impact of the East Asian monsoon rainfall changes on the erosion of the Mekong River basin over the past 25,000 yr. *Marine Geology* 271, 84–92. <https://doi.org/10.1016/j.margeo.2010.01.013>.
- He, Z.D., Liu, Z.F., Li, J.R., Xie, X., 2012. Elemental geochemical records in the western South China Sea since 540 ka and their paleoenvironmental implications (in Chinese). *Advances in Earth Science* 27, 327–336.
- Huang, J., Jiang, F., Wan, S., Zhang, J., Li, A., Li, T., 2016. Terrigenous supplies variability over the past 22,000 yr in the southern South China Sea slope: Relation to sea level and monsoon rainfall changes. *Journal of Asian Earth Sciences* 117, 317–327.
<https://doi.org/10.1016/j.jseaes.2015.12.019>.
- Jian, Z.M., Huang, B.Q., Kuhnt, W., Lin, H.L., 2001. Late Quaternary upwelling intensity and East Asian Monsoon forcing in the South China Sea. *Quaternary Research* 55, 363–370.
<https://doi.org/10.1006/qres.2001.2231>.
- Jiwarungrueangkul, T., Liu, Z., Zhao, Y., 2019a. Terrigenous sediment input responding to sea level change and East Asian monsoon evolution since the last deglaciation in the southern South China Sea. *Global and Planetary Change* 174, 127–137.
<https://doi.org/10.1016/j.gloplacha.2019.01.011>.
- Jiwarungrueangkul, T., Liu, Z., Stattegger, K., Sang, P.N., 2019b. Reconstructing chemical weathering intensity in the Mekong River basin since the Last Glacial Maximum. *Paleoceanography and Paleoclimatology* 34, 1–16.
<https://doi.org/10.1029/2019PA003608>.
- Laj C., Wang P.X., Balut Y., et al., 2005. MD147-Marco Polo Images XII Cruise Report. Brest: Institut Polaire Français, pp. 149.

- Li, Y.H., Schoonmaker, J.E., 2003. Chemical composition and mineralogy of marine sediments. In: F.T Mackenzie (Ed.), *Sediments, diagenesis, and sedimentary rocks. Treatise on geochemistry*, 7, pp. 35. <https://doi.org/10.1016/B0-08-043751-6/07088-2>.
- Liu, Z., Trentesaux, A., Clemens, S.C., Colin, C., Wang, P., Huang, B., Boulay, S., 2003. Clay mineral assemblages in the northern South China Sea: Implications for East Asian monsoon evolution over the past 2 million years. *Marine Geology* 201, 133–146. [https://doi.org/10.1016/S0025-3227\(03\)00213-5](https://doi.org/10.1016/S0025-3227(03)00213-5).
- Liu, Z., Colin, C., Trentesaux, A., Blamart, D., Bassinot, F., Siani, G., Sicre, M., 2004. Erosional history of the eastern Tibetan Plateau since 190 kyr ago: Clay mineralogical and geochemical investigations from the southwestern South China Sea. *Marine Geology* 209, 1–18. <https://doi.org/doi:10.1016/j.margeo.2004.06.004>.
- Liu, Z., Colin, C., Trentesaux, A., Siani, G., Frank, N., Blamart, D., Farid, S., 2005. Late Quaternary climatic control on erosion and weathering in the eastern Tibetan Plateau and the Mekong Basin. *Quaternary Research* 63, 316–328. <https://doi.org/10.1016/j.yqres.2005.02.005>.
- Liu, Z., Colin, C., Huang, W., Phon, L.K., Tong, S., Chen, Z., Trentesaux, A., 2007a. Climatic and tectonic controls on weathering in south China and Indochina Peninsula: clay mineralogical and geochemical investigations from the Pearl, Red, and Mekong drainage basins. *Geochemistry, Geophysics, Geosystems* 8, 1–18. <https://doi.org/10.1029/2006GC001490>.
- Liu, Z., Zhao, Y., Li, J., Colin, C., 2007b. Late Quaternary clay minerals off Middle Vietnam in the western South China Sea: Implications for source analysis and East Asian monsoon evolution. *Science in China Series D-Earth Sciences* 50, 1674–1684. <https://doi.org/10.1007/s11430-007-0115-8>.
- Liu, Z., Wang, H., Hantoro, W.S., Sathiamurthy, E., Colin, C., Zhao, Y., Li, J., 2012. Climatic and tectonic controls on chemical weathering in tropical Southeast Asia (Malay Peninsula,

- Borneo, and Sumatra). *Chemical Geology* 291, 1–12.
<https://doi.org/10.1016/j.chemgeo.2011.11.015>.
- Liu, Z., Zhao, Y., Colin, C., Stattegger, K., Wiesner, M.G., Huh, C., Zhang, Y., Li, X.,
 Sompongchaiyakul, P., You, C., Huang, C., Liu, J.T., Siringan, F.P., Phon, K.,
 Sathiamurthy, E., Hantoro, W.S., Liu, J., Tuo, S., Zhao, S., Zhou, S., He, Z., Wang, Y.,
 Bunsomboonsakul, S., Li, Y., 2016. Source-to-sink transport processes of fluvial
 sediments in the South China Sea. *Earth-Science Reviews* 153, 238–273.
<https://doi.org/10.1016/j.earscirev.2015.08.005>.
- McLennan, S.M., 1993. Weathering and global denudation. *The Journal of Geology* 101, 295–
 303. <https://doi.org/10.1086/648222>.
- Milliman, J.D., Syvitski, J.P.M., 1992. Geomorphic/tectonic control of sediment discharge to the
 ocean: the importance of small mountainous rivers. *The Journal of Geology* 100, 525–
 544. <https://doi.org/10.1086/629606>.
- Milliman, J.D., Farnsworth, K.L., 2011. River discharge to the coastal ocean-A global synthesis.
 Cambridge University Press, Cambridge, pp. 382.
<https://doi.org/10.5670/oceanog.2011.108>.
- Nesbitt, H.W., Markovics, G., Price, R.C., 1980. Chemical processes affecting alkalis and
 alkaline Earth during continental weathering. *Geochimica et Cosmochimica Acta* 44,
 1659–1666. [https://doi.org/10.1016/0016-7037\(80\)90218-5](https://doi.org/10.1016/0016-7037(80)90218-5).
- Nesbitt, H.W., Young, G.M., 1982. Early Proterozoic climates and plate motions inferred from
 major element chemistry of lutites. *Nature* 299, 715–717.
<https://doi.org/10.1038/299715a0>.
- Nesbitt, H.W., Young, G.M., 1984. Prediction of some weathering trends of plutonic and
 volcanic rocks based on thermodynamic and kinetic considerations. *Geochimica et*
Cosmochimica Acta 48, 1523–1534. [https://doi.org/10.1016/0016-7037\(84\)90408-3](https://doi.org/10.1016/0016-7037(84)90408-3).

- Nesbitt, H.W., Young, G.M., 1989. Formation and diagenesis of weathering profiles. *The Journal of Geology* 97, 129–147. <https://doi.org/10.1086/629290>.
- Nesbitt, H.W., Young, G.M., McLennan, S.M., Keays, R.R., 1996. Effects of chemical weathering and sorting on the petrogenesis of siliciclastic sediments, with implications for provenance studies. *The Journal of Geology* 104, 525–542. <https://doi.org/10.1086/629850>.
- Sang, P.N., Liu, Z., Stattegger, K., 2019. Weathering and erosion in central Vietnam over the Holocene and Younger Dryas: Clay mineralogy and elemental geochemistry from the Vietnam Shelf, western South China Sea. *Journal of Asian Earth Sciences* 179, 1–10. <https://doi.org/10.1016/j.jseaes.2019.04.008>.
- Taylor, S.R., McLennan, S.M., 1985. *The continental crust: Its composition and evolution*. Blackwell, Malden, Mass, pp. 312. <https://doi.org/10.1002/gj.3350210116>.
- Wan, S., Li, A., Clift, P.D., Stuut, J.-B.W., 2007. Development of the East Asian monsoon: Mineralogical and sedimentologic records in the northern South China Sea since 20 Ma. *Paleogeography, Palaeoclimatology, Palaeoecology* 254, 561–582. <https://doi.org/10.1016/j.palaeo.2007.07.009>.
- Wang, P., Wang, L., Bian, Y., Jian, Z., 1995. Late Quaternary paleoceanography of the South China Sea: Surface circulation and carbonate cycles. *Marine Geology* 127, 145–165. [https://doi.org/10.1016/0025-3227\(95\)00008-M](https://doi.org/10.1016/0025-3227(95)00008-M).
- Webster, P.J., 1994. The role of hydrological processes in ocean-atmosphere interactions. *Reviews of Geophysics* 32, 427–476. <https://doi.org/10.1029/94RG01873>.
- Zhang, W., Wei, X.Y., Zheng, J.H., Zhu, Y.L., Zhang, Y.J., 2012. Estimating suspended sediment loads in the Pearl River Delta region using sediment rating curves. *Continental Shelf Research* 38, 35–46. <https://doi.org/10.1016/j.csr.2012.02.017>.

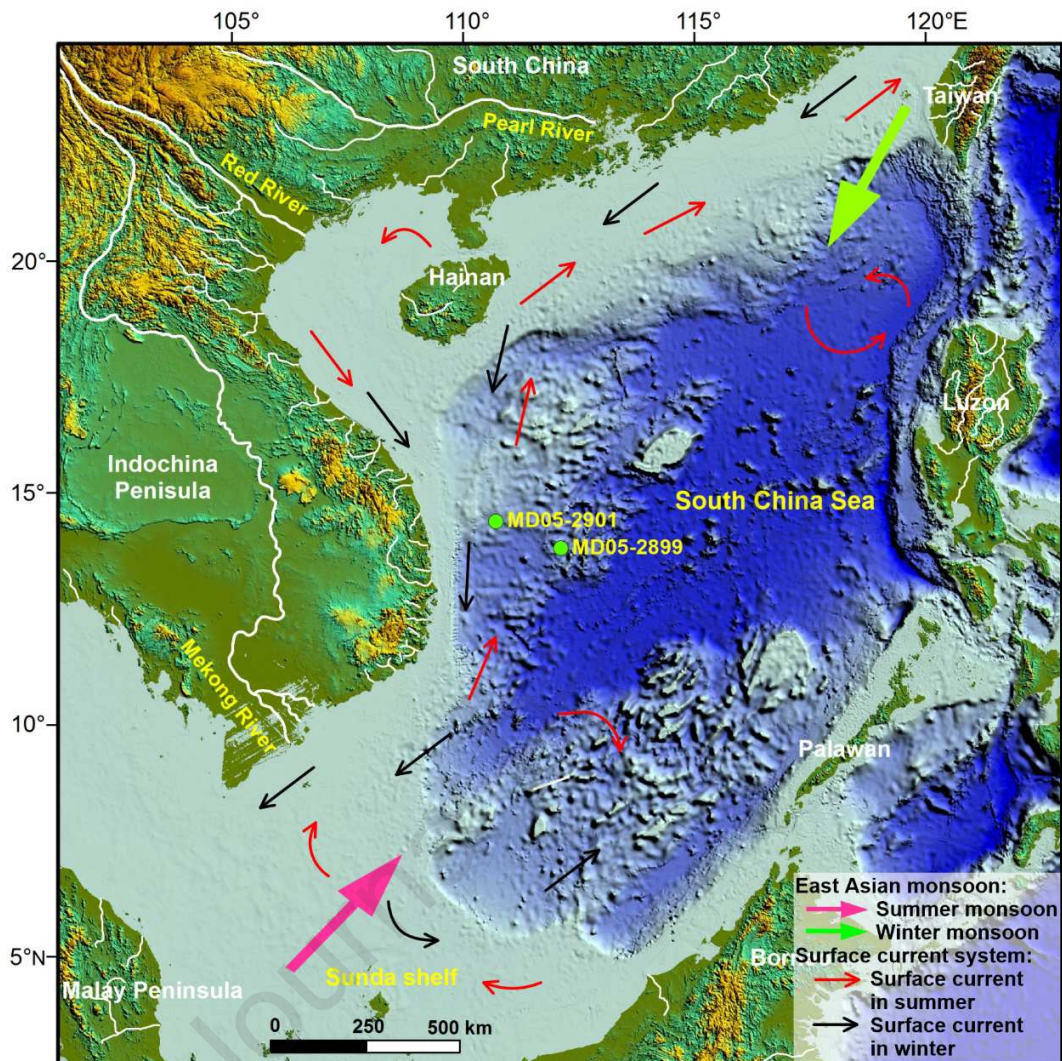


Figure 1. Geomorphological and bathymetric map of the South China Sea showing the location of Cores MD05-2899 and MD05-2901 off central Vietnam in the lower continental slope of the western South China Sea. Basic types of surface currents from Wang et al. (1995) and monsoon winds after Webster (1994).

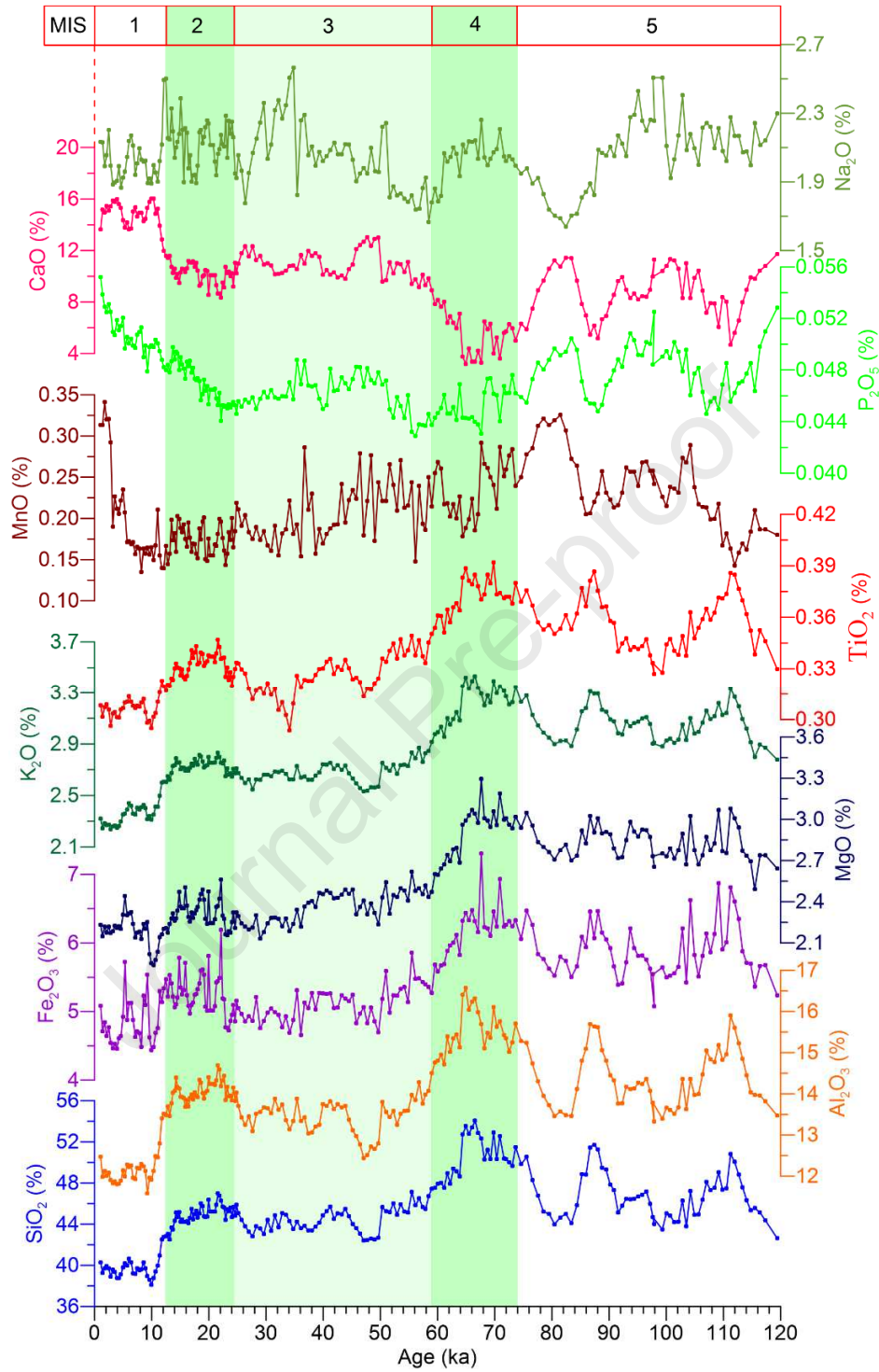


Figure 2. Temporal variations of major elements of Core MD05-2899 during the last glacial-interglacial cycle.

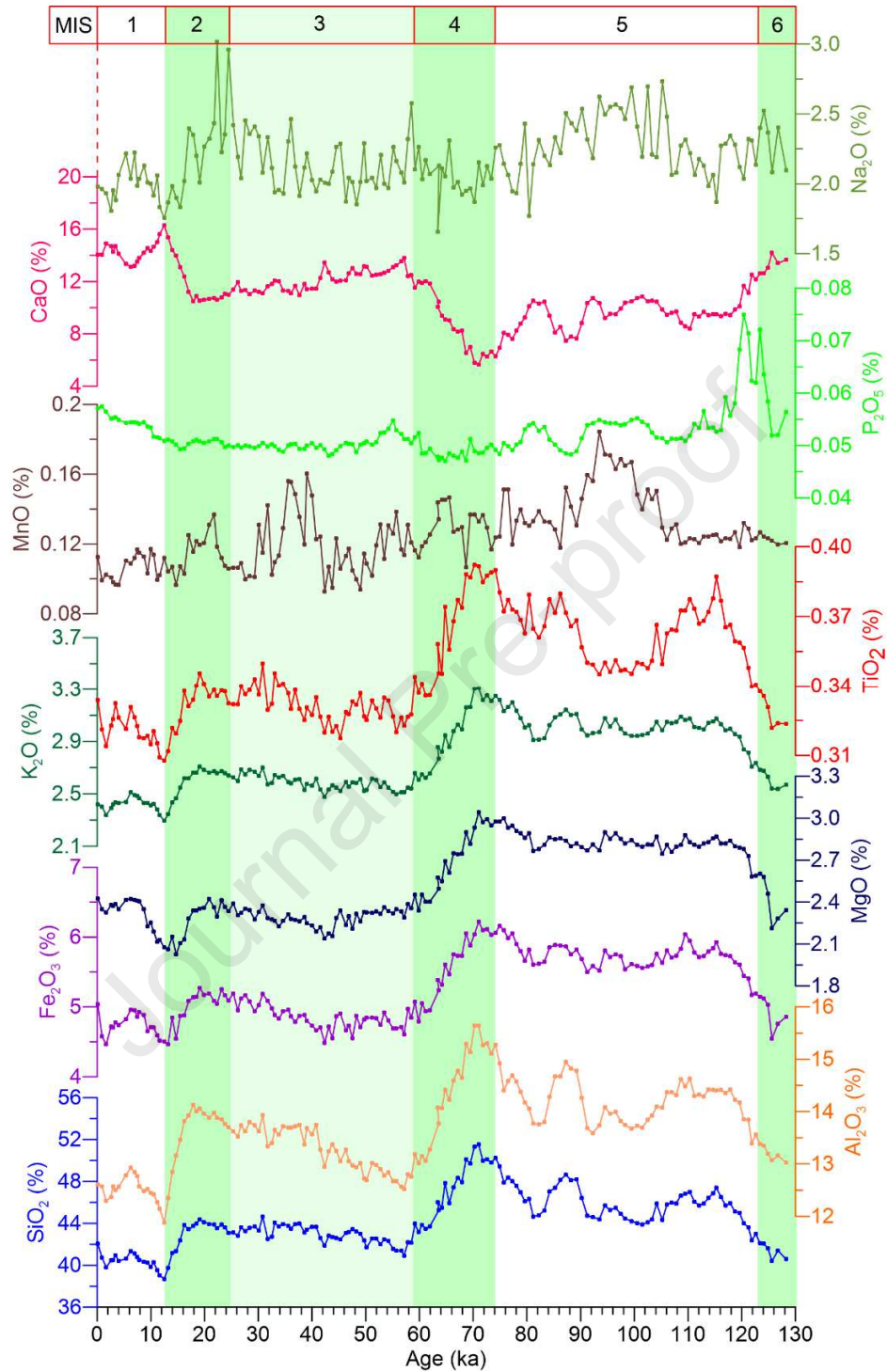


Figure 3. Temporal variations of major elements of Core MD05-2901 during the last glacial-interglacial cycle.

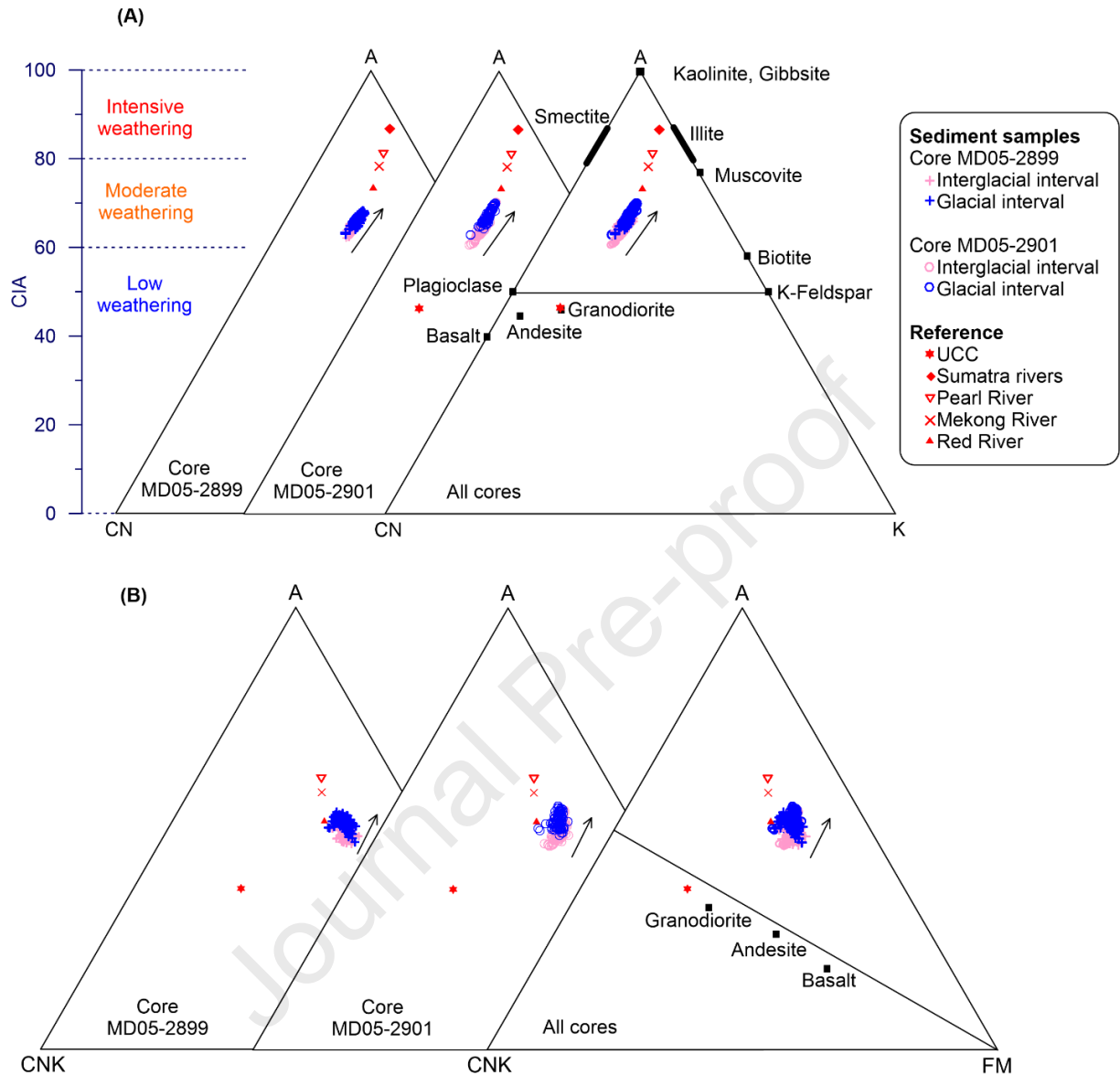


Figure 4. (A) CIA, A-CN-K, and (B) A-CNK-FM ternary diagrams of sediment samples at Cores MD05-2899 and MD05-2901 in the western South China Sea are plotted for comparison. A = Al_2O_3 ; C = CaO^* ; N = Na_2O ; K = K_2O , F = total Fe; M = MgO. Average data of Pearl, Mekong, and Red rivers (Liu et al., 2007a) and Sumatra rivers (Liu et al., 2012) are plotted for comparison; UCC (Taylor and McLennan, 1985) was plotted as a reference value. Arrows display movements of major elements.

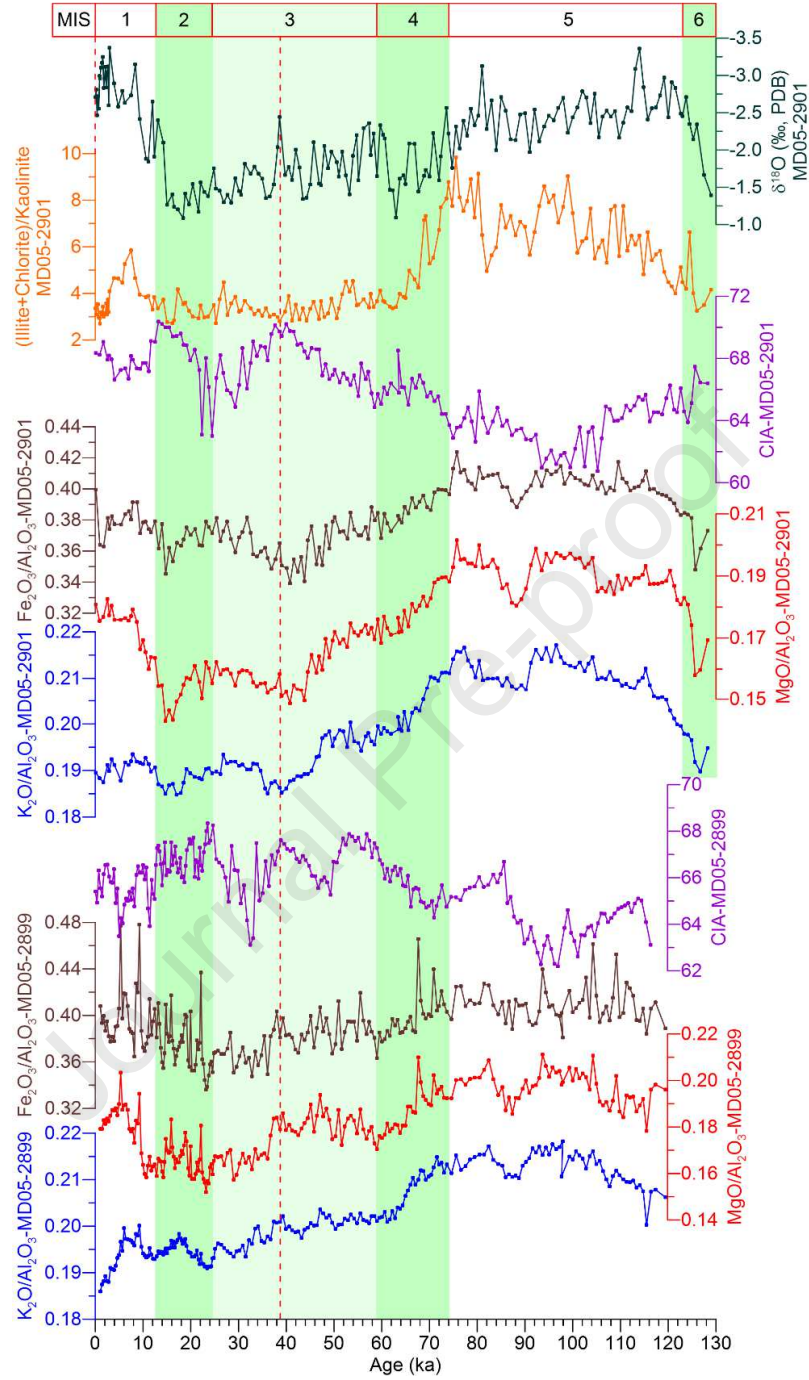


Figure 5. Comparison of K_2O/Al_2O_3 , MgO/Al_2O_3 , Fe_2O_3/Al_2O_3 , and CIA at Cores MD05-2899 and MD05-2901, with paleoclimatic records and proxies. Planktonic foraminifera *G. ruber* $\delta^{18}O$ records and (illite + chlorite)/kaolinite at Core MD05-2901 from Liu et al. (2007b). Red dashed line in the middle of MIS 3 shows strong variations in our elemental proxies.

Declaration of interests

☒ The authors declare that they have no known competing financial interests or personal relationships that could have appeared to influence the work reported in this paper.

☐ The authors declare the following financial interests/personal relationships which may be considered as potential competing interests: